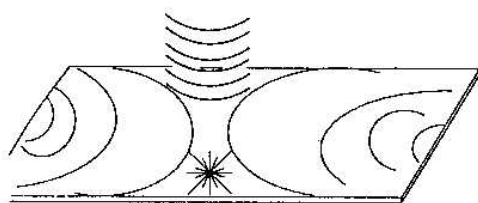


# AIP CONFERENCE PROCEEDINGS 298

## ULTRAFAST REACTION DYNAMICS AND SOLVENT EFFECTS

ROYAUMONT, FRANCE 1993



**EDITORS:**

**YANN GAUDUEL**

ÉCOLE POLYTECHNIQUE-ENSTA

**PETER J. ROSSKY**

UNIVERSITY OF TEXAS AT AUSTIN

**AIP  
PRESS**

American Institute of Physics

New York

## NMR STUDIES OF ELEMENTARY STEPS OF HYDROGEN TRANSFER IN CONDENSED PHASES

H.H.Limbach, G.Scherer L.Meschede, F. Aguilar-Parrilla  
B.Wehrle, J.Braun, Ch.Hoelger, H.Benedict, G.Buntkowsky  
W.P.Fehlhammer  
Fachbereich Chemie, Freie Universität Berlin, W-1000 Berlin 33,  
F.R.G.

J.Elguero  
Instituto de Quimica Medica CSIC, E-28006 Madrid, Spain

J.A.S.Smith  
King's College, Dept. of Chemistry, Strand, London WC2R 2LS, England

B.Chaudret  
Laboratoire de Chimie de Coordination du CNRS,  
F-31077 Toulouse-Cedex, France

### ABSTRACT

In this paper recent developments and results of dynamic high resolution NMR spectroscopy in the study of elementary steps of proton transfers in liquids and solids are reviewed.

### INTRODUCTION

During the past decade, NMR spectroscopy has developed into a powerful kinetic tool in the study of hydrogen and deuterium transfers in liquids.<sup>1-11</sup> This method is based on the modulation of isotropic chemical shifts and scalar coupling constants occurring during these processes. The latter may also modulate other nuclear interactions, a phenomenon which has been used to study rapid proton and deuteron transfers in solids.<sup>12-15</sup> The development of high resolution solid state NMR spectroscopy of spin 1/2 nuclei under the conditions of magic angle spinning (MAS), <sup>1</sup>H decoupling and <sup>1</sup>H cross polarization (CP)<sup>16</sup> has made it also possible to monitor solid state chemical shift modulations. Using this method, a variety of hydrogen transfers in solids has been detected.<sup>14,24</sup> Advantages of solid state NMR methods are the wider dynamic range as compared to liquid state NMR and the possibility of studying models for reactive hydrogen transfer complexes in a timescale of slow molecular motions, a goal which is difficult to achieve by liquid state NMR.

The purpose of this paper is to review these recent developments in dynamic high resolution NMR spectroscopy. The first section deals with NMR studies of multiple kinetic hydrogen/deuterium isotope effects and the following sections with solid state effects on proton transfers in ordered and disordered solids. In particular, hydrogen transfers between nitrogen atoms are considered which can conveniently be monitored by <sup>15</sup>N CPMAS NMR of the <sup>15</sup>N labeled compounds. In addition, an extension of the method into the nano-second timescale is described. The possibility of studying proton motions in strong ionic hydrogen bonds by <sup>15</sup>N NMR is then discussed and a scenario of hydrogen transfer in condensed phases is described. Finally, the problem of coherent versus incoherent hydrogen tunneling in polyatomic molecules is discussed. This phenomenon plays a role in hydrogen exchange in transition metal hydrides,<sup>25-30</sup> monitored by liquid state NMR.

# NMR STUDIES OF MULTIPLE KINETIC HYDROGEN/DEUTERIUM ISOTOPE EFFECTS

The NMR methods for measuring rate constants of hydrogen transfer including their kinetic isotope effects have been reviewed recently.<sup>1</sup> Therefore, only some of the typical results obtained by this method are described here. As an example of an intramolecular double proton transfer system let us discuss the oxalamidine tautomerism which was discovered some years ago.<sup>6</sup> Fig.1 shows the Arrhenius curves of the HH-, HD-, and DD-reactions of the bicyclic oxalamidine OA7 dissolved in methylcyclohexane (MCY) and acetonitrile (AN). At 298K, a 5.4 fold increase of the rate constants is observed when replacing MCY by AN. This result indicates a highly polar transition state of the reaction, which is only in agreement with the stepwise reaction pathway but not with the concerted pathway shown in Fig. 1. The observed kinetic isotope effects point in the same direction. The HH/HD isotope effects are much larger than 1 because a single proton is in flight in the rate limiting step; the second mobile proton is still bound and contributes only a very small secondary isotope effect. The HD/DD isotope effect mainly arises from a symmetry factor present in the HH- and DD- but absent in the HD reaction. These results represent a strong deviation from the so-called rule of the geometric mean (RGM) which assumes that the HH/HD- and the HD/DD isotope effects are much alike. Similarly, a number of different degenerate and quasi-degenerate intra- and intermolecular double proton transfer reactions were also studied.<sup>1-11</sup>

As an example of an intermolecular double proton transfer, let us consider the case of di-(p-fluorophenyl)-formamidine (DFFA) dissolved in tetrahydrofuran.<sup>9</sup> In spite of difficulties arising from rapid hydrogen bond equilibria, it was possible to determine the rate constants of the double proton transfer in the cyclic dimer. The Arrhenius diagram obtained is shown in Fig 2a. In contrast

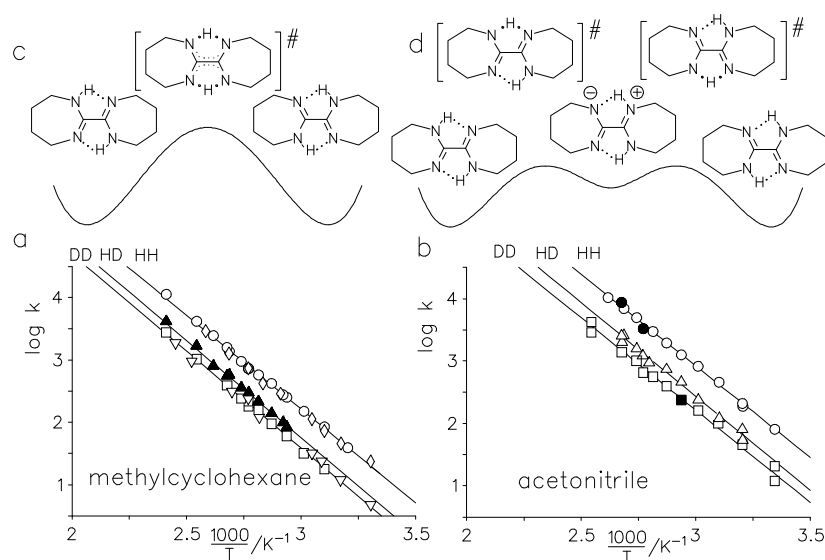


Fig.1. Arrhenius diagrams of the tautomerism of OA7 in methylcyclohexane (a) and acetonitrile (b). Concerted (c) and stepwise (d) proton transfer pathways. Reproduced from Ref. 7

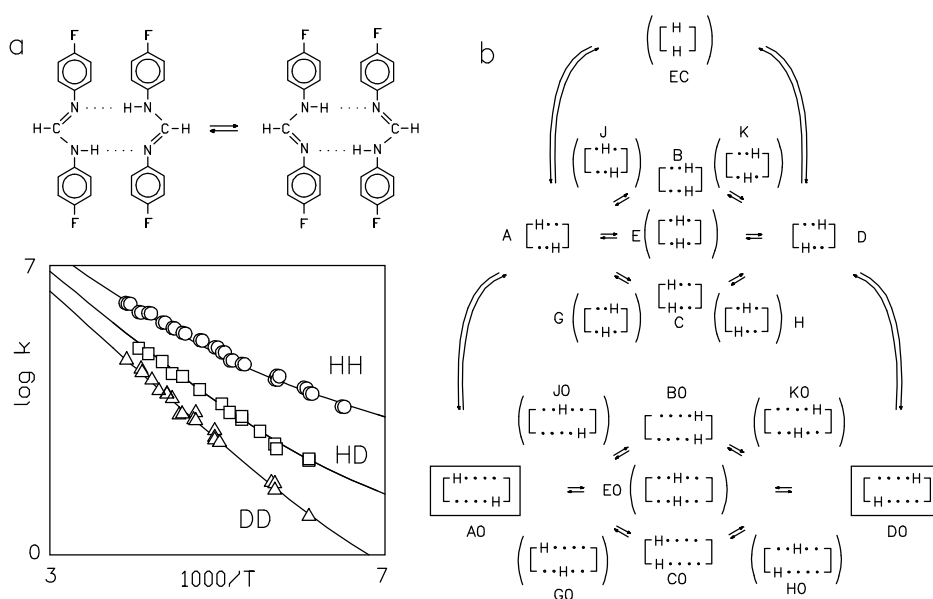


Fig.2. a: Arrhenius diagram of the double proton transfer in cyclic dimers of di-(p-fluorophenyl)formamidine dissolved in tetrahydrofuran. b: Convergence of the stepwise and the concerted reaction pathways by hydrogen bond compression. Adapted from Ref. 9.

to the intramolecular case now both the HH/HD and HD/DD isotope effects are large, although there is a deviation from the RGM. In terms of conventional transition state theory, this finding would indicate that the zero point energy of all mobile protons is reduced in the transition state as expected for a concerted reaction pathway or for a stepwise pathway where the vibrational frequencies of the bound proton are strongly reduced. This reduction may be caused by hydrogen bond compression in the transition state as illustrated in Fig.2b. In the strong hydrogen bond compression limit, the difference between the concerted and stepwise reaction mechanism eventually disappears. At lower temperatures, tunneling of the protons through the barrier may become important. According to Bell<sup>31</sup> this phenomenon leads to positive deviations from a linear Arrhenius law, as indicated by the solid lines in Fig.2a, calculated in terms of a modified Bell tunneling model. Unfortunately, measurements of rate constants in a larger temperature range will be necessary in order to confirm the proposed deviations and the contribution of tunneling.

This goal was achieved in the case of solid pyrazoles where some derivatives form cyclic dimers, trimers or tetramers in the crystalline state according to Fig.3a. In these complexes degenerate multiple hydrogen transfer processes could be detected by solid state  $^{15}\text{N}$  CPMAS NMR spectroscopy of the  $^{15}\text{N}$  labeled solids.<sup>20-22</sup> Problems with hydrogen bond equilibria are now absent. For solid 3,5-dimethylpyrazole, it was possible to obtain the HHH/HHD/HDD/DDD isotope effects as shown in Fig.3b. As in the case of DFFA at high temperatures almost equal HHH/HHD-, and HDD/DDD isotope effects are observed. However, low-temperature "magnetization transfer" experiments<sup>17</sup> at

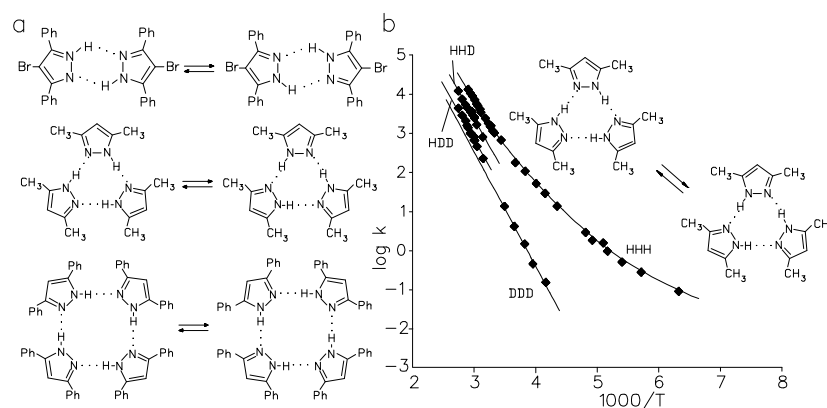


Fig.3. Tautomerism of pyrazoles in the solid state. Arrhenius diagram of the degenerate triple proton transfer in crystalline 3,5-dimethylpyrazole.<sup>22</sup>

low temperature indicated a non-Arrhenius behavior of the HHH reaction and a similar reaction pathway as in the case of DFFA. Further studies are underway in order to obtain information on the dependence of the kinetic isotope effects on the on the number of protons transferred.

In the future, it would be desirable to calculate Arrhenius curves of the type shown in Figs. 1-3 “ab initio“, including both the classical over-barrier and the low temperature tunneling regime. This task represents a major goal in theoretical chemistry. Several approaches have been proposed whose discussion is, however, beyond the scope of this paper. As examples we refer to Refs.12, 31, and 32. We will return to this problem in the final sections.

#### SOLID STATE EFFECTS ON DEGENERATE HYDROGEN TRANSFER REACTIONS IN CRYSTALLINE SOLIDS

In order to discuss the possibilities of high resolution solid state NMR for the study of solid state effects on hydrogen transfer reactions, we consider the tautomerism of <sup>15</sup>N labeled tetraphenylporphyrin (TPP). This compound was the first molecule for which an intramolecular hydrogen transfer has been detected by NMR, both in the liquid<sup>4</sup> and in the solid state.<sup>14</sup> In Fig.4 the superposed experimental and calculated spectra of <sup>15</sup>N labeled TPP in the tetragonal and the triclinic phase are compared.<sup>5</sup> Tetragonal TPP was prepared by co-crystallization with 10% w/w non-labeled Ni-TPP. At low temperatures, two sharp <sup>15</sup>N signals are observed indicating the presence of two different types of nitrogen atoms. The high field line stems from the protonated nitrogen atoms, the low field line from the non-protonated nitrogen atoms. As the temperature is increased line broadening is observed and coalescence into one single sharp center line occurs. Thus, at high temperatures, only one type of nitrogen atoms with an average proton density of 1/2 is observed. In other words, the equilibrium constant of the tautomerism is 1. By contrast, when the site symmetry of the molecule is reduced as in triclinic TPP, two lines are observed in the fast exchange regime which move towards each other as the temperature is further increased. This observation indicates the presence of two types of nitrogen atoms also at higher temperatures, one with a higher and the other with a lower average temperature dependent

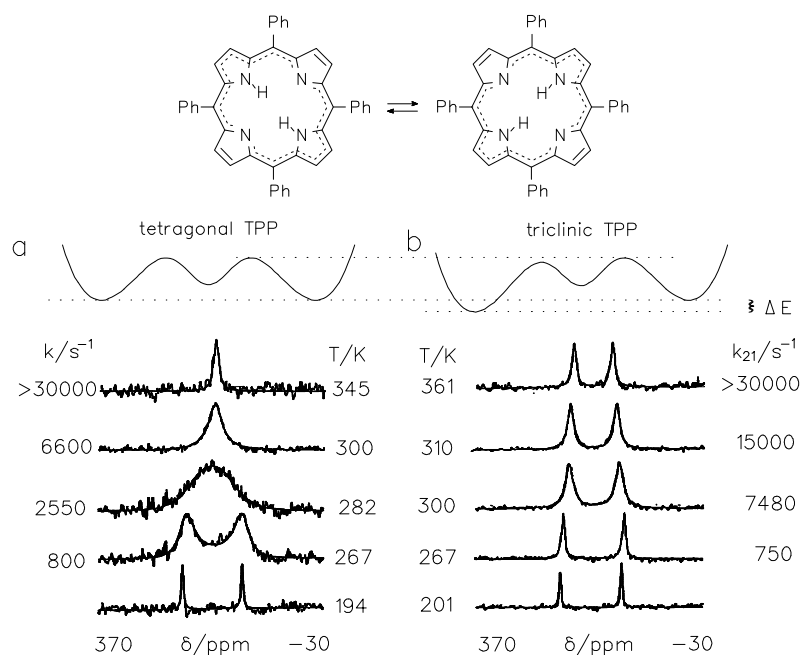


Fig.4. Superposed experimental and theoretical  $^{15}\text{N}$  CPMAS NMR spectra of TPP in the solid state. a: tetragonal TPP. b: triclinic TPP. Reproduced with permission from Ref (5)

proton density. The equilibrium constants of tautomerism and the energy difference between the tautomers could be obtained from the line splittings.<sup>5</sup>

The rate constants of the tautomerism in tetragonal TPP are almost the same as for TPP dissolved in organic liquids.<sup>5</sup> In other words, the main solid state effect on the tautomerism of TPP is the lifting of the degeneracy of the tautomers as illustrated schematically in Fig.4b.

#### INCREASE OF THE DYNAMIC RANGE OF HIGH RESOLUTION SOLID STATE NMR

As can be inferred from Fig.4  $^{15}\text{N}$  CPMAS NMR line shape analysis is a valuable tool only for the millisecond to microsecond time scale. By analysis of longitudinal  $^1\text{H}$  - or  $^2\text{H}$ - relaxation times  $T_1$  of solid hydrogen transfer systems, the dynamic range of NMR can be extended if the equilibrium constants of the tautomerism are known from independent measurements.<sup>10-12</sup> Up to now, this goal has only been achieved in studies of single crystals.<sup>10-12</sup> Here, we show that it is also possible to extend the method to crystalline powders by employing MAS conditions.

The system studied in  $^{15}\text{N}$  enriched dimethyltetraaza[14]annulene (DTAA, Fig.5) which is subject to the solid state tautomerism shown in Fig. 5.<sup>16-18</sup> The  $^{15}\text{N}$  CPMAS NMR spectra<sup>23</sup> (Fig.5a) exhibit similar features to those of triclinic TPP. In particular, the decrease of the line splitting at room temperature with increasing temperature is well pronounced, arising from the increase of the equilibrium constant of tautomerism between the two tautomers. The latter are

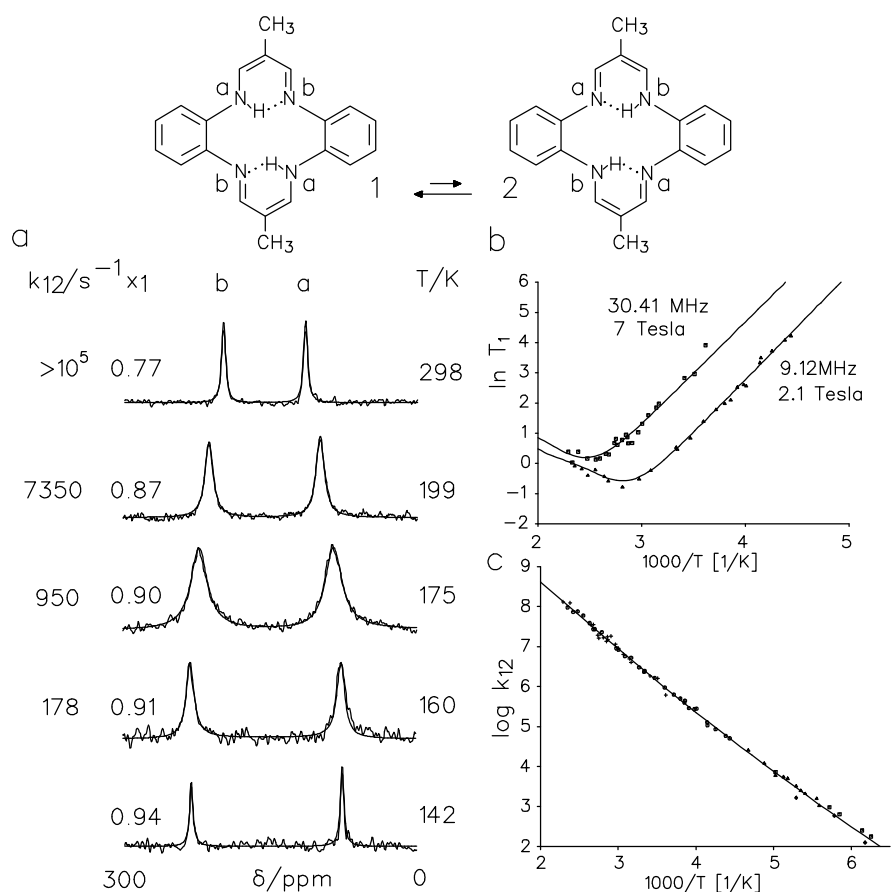


Fig.5. a: Superposed experimental and theoretical  $^{15}\text{N}$  CPMAS NMR spectra of crystalline DTAA. b:  $^{15}\text{N}$ - $T_1$  analysis. c: Arrhenius diagram.<sup>23</sup>

non-degenerate in the crystalline state. The maximum rate constant which could be determined by lineshape analysis was approx.  $10^4 \text{ s}^{-1}$ . The longitudinal  $^{15}\text{N}$   $T_1$  relaxation times were measured in the usual way under MAS conditions and plotted in Fig. 5b as a function of the inverse temperature, at two different magnetic field strengths  $B_0$ . The source of the relaxation lies in the dipolar interaction between  $^{15}\text{N}$  nuclei probed and the mobile protons modulated by the proton transfer. A  $T_1$ -minimum occurs when the inverse correlation time  $\tau$  of the proton motion is of the order of the  $^{15}\text{N}$  Larmor-frequency. Since  $\tau$  decreases with temperature, the minimum appears at higher temperatures when  $B_0$  is increased. From the value of  $T_1$  in the minimum, the NH-distance is obtained. With the knowledge of the equilibrium constants from the line positions it was possible to convert the  $T_1$  values into forward rate constants  $k_{12}$  of proton transfer as shown in Fig. 5c. The rate constants obtained in this way are now in the nanosecond range and agree well with those obtained at low temperature by lineshape analysis. This result represents a considerable increase of the timescale of high resolution solid state NMR. The data in Fig. 5c indicate a slight deviation from an Arrhenius behavior which could arise from tunneling. In principle, it should be possible to reach the picosecond timescale when studying systems with lower energy of activation of proton transfer in the future.

### SOLID STATE EFFECTS ON DEGENERATE HYDROGEN TRANSFER REACTIONS IN DISORDERED SOLIDS

So far, we have considered crystals where the different molecules experience the same forward and backward rate constants, and, therefore also the same equilibrium constants of tautomerism. What however will happen to the proton transfer systems when they are dissolved in a glass or a liquid which provides a broad distribution of different molecular environments?

In order to study these questions  $^{15}\text{N}$  CPMAS NMR experiments have been performed on various  $^{15}\text{N}$  labeled dyes embedded in glassy solids or in amorphous environments.<sup>18</sup> We omit a detailed description of the spectral results obtained but discuss only the model which was used in order to simulate the experimental  $^{15}\text{N}$  NMR lineshapes. This model is illustrated in Fig 6. A molecule which forms two degenerate tautomers in the gasphase where the conversion can be described in terms of a symmetric double minimum potential is considered. As shown in the preceding section the degeneracy will be lifted in an ordered solid as shown in Fig. 6a. As long as intermolecular interactions are small all molecules will experience the same slightly asymmetric potential of the proton motion. By contrast in a disordered solid like a glass there will be a broad distribution of different environments characterized by different rate and equilibrium constants of proton transfer. Exchange between different sites is very slow in the NMR timescale. The situation can be described as a static superposition of local potential curves. At the glass transition, molecular motions caused by solvent reorientation and relaxation becomes important leading to site exchange or in other words to a time-dependent fluctuation of the potential. This motional averaging process restores the symmetry of the effective double minimum, in the timescale of NMR. However, the actual proton transfer steps are independent of the solvent relaxation. In the examples studied<sup>18</sup> the NMR spectra were compatible with a gaussian distribution of energy differences between the tautomers. Such a distribution has been postulated recently on theoretical grounds.<sup>32</sup>

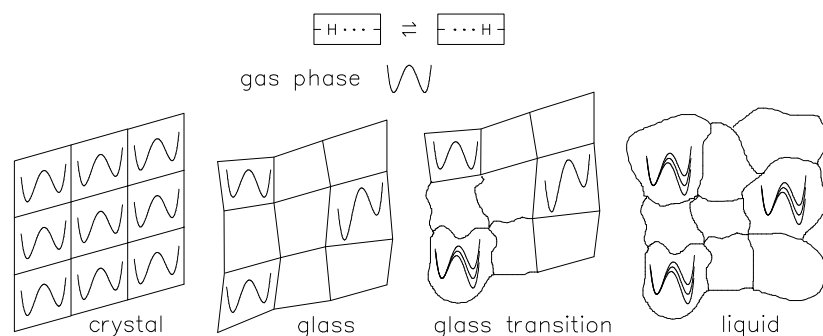


Fig 6. Model for the dependence of the proton transfer potential on the environment arising from experimental observations.<sup>18</sup>

### SOLID STATE EFFECTS ON STRONG HYDROGEN BONDS IN ORGANIC SOLIDS

In the previous sections only neutral hydrogen transfer systems involving relatively large transfer barriers were considered. The problem of charge transfer



associated usually with proton transfer was therefore eliminated. Because of this complication, proton transfers in liquids are generally very complex as illustrated schematically in Fig. 7a for the simple degenerate proton transfer between an acid AH and its conjugate base  $A^-$ . The solvent is more ordered around  $A^-$  than around AH because of strong ion-dipole interactions. Two situations can arise if the encounter complex is formed. In the case where the complex is characterized by a weak hydrogen bond, proton transfer is characterized by a barrier. As inferred from the previous section the barrier parameters are modulated in different solvation sites. Proton transfer mostly takes place in environments characterized by asymmetric double minimum potentials. Solvent relaxation restores the optimum solute solvent interaction. Both processes are statistically independent. The average perturbation of the double minimum potentials can be much larger as compared to the neutral systems of the preceding sections. By contrast if a very strong hydrogen bond is formed in the encounter complex, the proton transfer potential may be barrierless i.e. characterized by a more or less asymmetric single minimum potential. Depending on the solvent molecules, the proton is located somewhere in the hydrogen bond. The transfer of the proton is now strongly coupled to solvent relaxation. In other words, solvent reorientation induces the proton transfer. Proton transfer systems of this type generally exhibit strong continua in the IR spectra<sup>33</sup> from which interesting information concerning the proton dynamics can be derived. Here, we show that high resolution solid state NMR can contribute interesting information concerning the proton position in extremely strong hydrogen bonds.

The example studied is a solid salt of the type  $AHA^+K^+$ , its structure is shown in Fig. 7b. The hydrogen bond proton is located somewhere in between two  $^{15}N$  atoms which are only 2.54 Å apart.<sup>24</sup> At the top, the  $^{15}N$  CPMAS NMR spectra of the separate solid reactants AH and  $A^+K^+$  are shown. AH exhibits a signal at 150 ppm and  $A^+$  a signal at ~ 290 ppm. When the reactants are allowed to cocrystallize to  $AHA^+K^+$  a single line at ~ 210 ppm is obtained when  $K^+ = AsPh_4$ , indicating a single type of nitrogen atom. The position of  $K^+$  is such that the hydrogen bond proton either jumps rapidly between two potential wells of equal energy or that it moves in a symmetric single well potential where the minimum is located midway between the two nitrogen atoms. By contrast, in the case of  $K^+ = NPr_4^+$ , two lines are observed at 190 and 220 ppm indicating that the hydrogen bond proton is displaced from the center position. In contrast to triclinic TPP and DTAA, the line splitting is almost independent of temperature as expected for an asymmetric single minimum potential. Therefore, the results shown in Fig. 7b indicate the presence of an asymmetric single minimum potential or of an asymmetric double minimum potential with an extremely small barrier, possibly smaller than the vibrational groundstate. Further studies are underway in order to characterize the proton positions, the potential of the proton motion and the vibrational wave functions, by studying the dipolar interaction of  $^{15}N$  with attached hydrogen isotopes. Note that information of this type can not easily be obtained by vibrational spectroscopy or by diffraction techniques. In summary, solid state NMR will be an interesting method for characterizing intermediate states of ionic proton transfer reactions in the future.

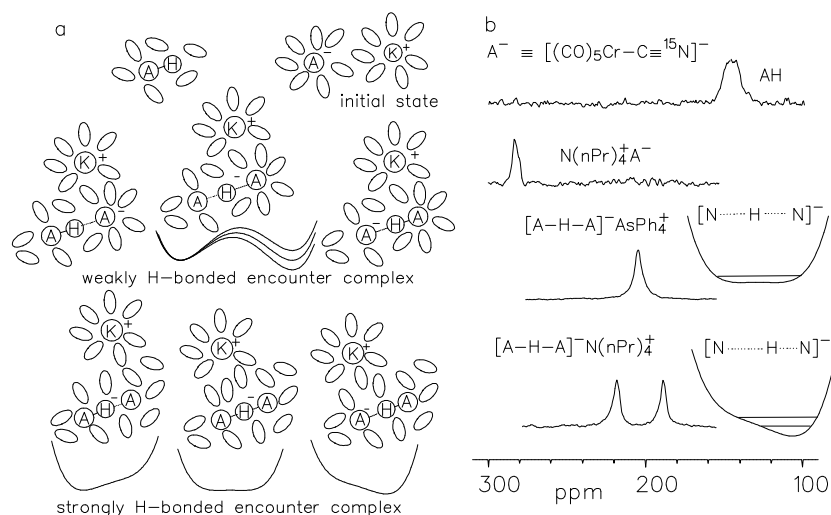


Fig. 7. a: Models of proton transfer in liquids. b:  $^{15}\text{N}$  CPMAS NMR study of frozen stages of proton transfer in a strong NHN hydrogen bond.<sup>24</sup>

### COHERENT HYDROGEN TUNNELING IN POLYATOMIC MOLECULES IN CONDENSED PHASES

At this stage, it is interesting to discuss the consequences of the results obtained in the preceding sections for the details of hydrogen transfer in condensed matter. Let us start with the simplest models proposed to accommodate degenerate hydrogen transfer processes, i.e. the theory of the one-dimensional symmetric double minimum potential.<sup>34</sup> As illustrated in Fig.8a, this model predicts delocalized vibrational hydrogen states which are given in approximation as the positive and the negative linear combinations of harmonic oscillator states. The energy splitting is  $\hbar J$ , where  $J$  can be interpreted as frequency of coherent hydrogen tunneling.<sup>34</sup> With the exception of some small molecules in the gas phase, this model could not be verified in the cases discussed above where the hydrogen transfer processes are stochastic i.e. characterized by a rate constant. The transition between the two regimes is one of the major problems in theoretical chemistry of reaction dynamics in polyatomic molecules embedded in condensed matter.<sup>32</sup> Here, we restrict ourselves to a qualitative explanation of these phenomena, based on experimental observations.

For the case where the gas phase symmetry of the double minimum potential is lifted in a crystal - as observed in the preceding sections - one-dimensional double oscillator theory predicts localized proton wave functions as illustrated in Fig.8b. In order to arrive at a rate process, more dimensions have to be taken into account.<sup>12/32</sup> The simplest process one can conceive is vibrational relaxation (VR) occurring in polyatomic molecules.<sup>35</sup> VR leads to a stochastic interchange between the localized states of Fig. 8b. However, VR is also present in the gasphase. When the rate constant of VR is of the order of  $J$ , the coherence of tunneling is destroyed and hydrogen transfer becomes an incoherent tunneling process at low temperatures and a classical over-barrier process at high temperatures. In the liquid state, the effective symmetry of the

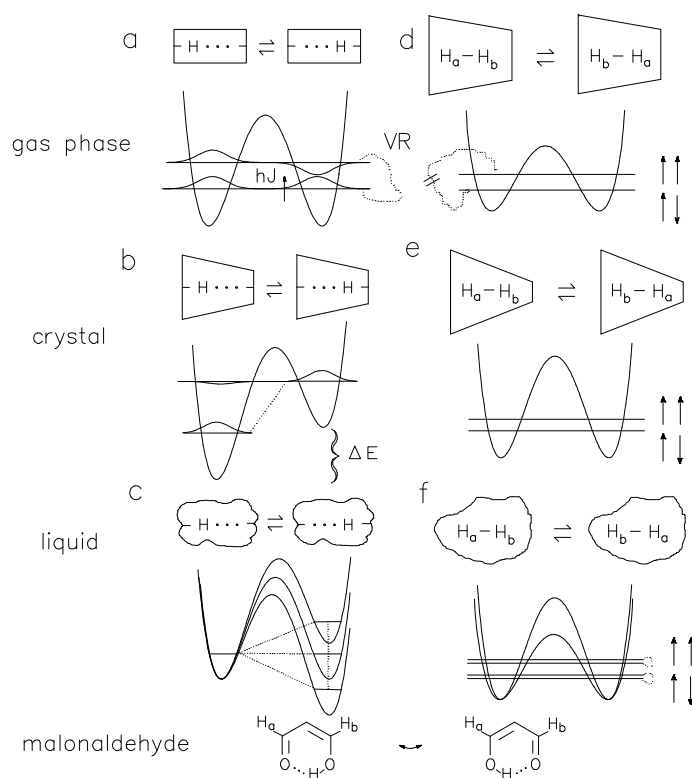


Fig.8. One-dimensional double oscillator models for hydrogen transfer and dihydrogen exchange under different conditions.

potential is restored by solvent relaxation and a smaller tunnel splitting could survive (Fig. 8c). However, VR leads again to a stochastic transfer process.

As illustrated in Fig.8d-e, there are, however, systems where coherent tunneling can survive VR and intermolecular interactions, e.g. the exchange of a pair of two hydrogen atoms in space. The potential curve of this process is shown in Fig. 8d for the gasphase. The nuclear spins - characterized by arrows - play now a decisive role. The lower tunnel state is symmetric with respect to a permutation  $H_a-H_b \rightarrow H_b-H_a$  and the upper state antisymmetric. Since hydrogen has a nuclear spin  $1/2$  the lower state has to be coupled with the antisymmetric nuclear spin function  $\uparrow\downarrow$  (antiparallel spin) in order to fulfill the Pauli exclusion principle. By contrast, the upper tunnel state is antisymmetric and has to be combined with the symmetric nuclear spin states  $\uparrow\uparrow$  (parallel spins), as in the case of  $o\text{-H}_2$  and  $p\text{-H}_2$ . Thus, interconversion of the delocalized dihydrogen states involves also a nuclear spin conversion which is much slower than VR. Thus, the tunnel splittings  $hJ$  can survive even in larger molecules, even in the NMR timescale. In the crystalline solid the barrier of interchange and the value of  $J$  may be altered but not the inherent symmetry of the process (Fig. 8e). When placing the molecule in a multitude of different exchanging environments, i.e. in a liquid (Fig. 8f) solvent relaxation will lead to an average temperature dependent tunnel splitting as long as nuclear spin conversion is slow.

Fig. 8d provides also an explanation for the observation that VR does not seem to be operative in the case of malonaldehyde (Fig. 8) in the gas phase.<sup>36</sup> For this molecule a ground state tunnel splitting has been observed.<sup>36</sup> In terms of its proton transfer features this molecule would range among the examples shown in Fig. 8a-c; however, in the gas phase this molecule is also of the type shown in Fig. 8d-f because of the two hydrogen atoms  $H_a$  and  $H_b$ . As shown in Ref. 36, the wave function in the gas phase can be approximated by the product

of the vibrational rotational and nuclear spin functions  $\Psi = \psi_v \psi_r \psi_s$ . According to the Pauli exclusion principle, the combinations ssa, sas, ass and aaa are possible where s = symmetric and a = antisymmetric with respect to the permutation  $H_a-H_b \rightarrow H_b-H_a$ . In the gas phase both rotational relaxation and nuclear spin relaxation is slow enabling the observation of tunnel splittings. By contrast, in condensed matter, a reduction of the molecular symmetry occurs<sup>37</sup> and the suppression of the molecular rotation leads to a spatial wave function which is neither symmetric nor antisymmetric with respect to the above mentioned permutation. As a consequence, symmetric and antisymmetric nuclear spin functions can be combined with all spatial functions. Nuclear spin relaxation is then no longer a bottleneck for vibrational relaxation between the two lowest vibrational states and coherent tunneling is destroyed. The same phenomenon could arise in the gas phase after substitution of  $H_a$  by deuterium. This substitution also reduces tunneling because of a reduction of the molecular symmetry.<sup>38</sup>

### COHERENT HYDROGEN TUNNELING IN TRANSITION METAL HYDRIDES

Coherent hydrogen tunneling in polyatomic molecules embedded in liquid, will then survive intermolecular interactions and VR only in the cases of mutual exchange of pairs of hydrogen atoms as shown in Fig. 8e-f. In fact, this phenomenon has recently been observed by NMR spectroscopy in a number of transition metal trihydrides and dihydrides, where it has been called "quantum exchange"<sup>25-30</sup> As an experimental introduction into this problem let us consider the case of an adduct of a Ru-trihydride with Cu.<sup>26</sup> The structure and the superposed experimental and calculated 500 MHz  $^1H$  spectra of this molecule dissolved in acetone- $d_6$  are shown in Fig. 9.<sup>39</sup> At low temperatures three signals are observed for the three hydride atoms  $H_a$ ,  $H_b$  and  $H_c$ . Signals b and c are split by coupling into doublets characterized by the coupling constant  $J_{bc}$ . A fluxional process which interconverts atoms a and c. At higher temperatures an

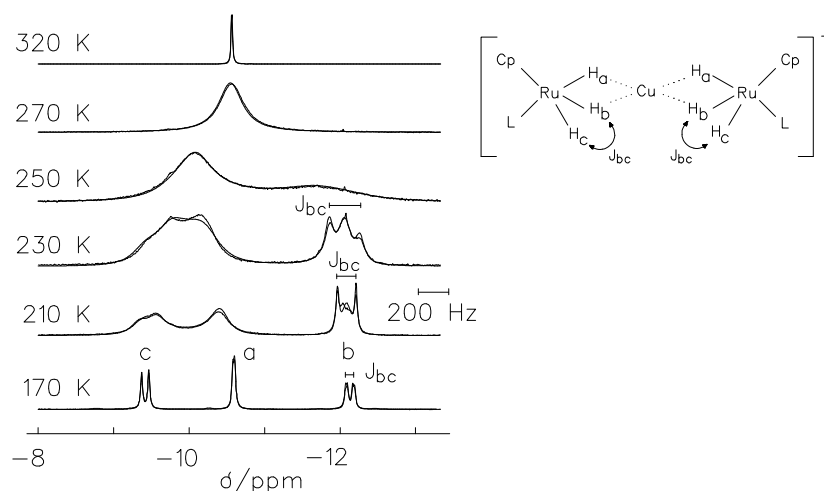


Fig.9. Superposed experimental and calculated 500 MHz  $^1H$  NMR spectra of a transition metal hydride dissolved in acetone- $d_6$ .<sup>39</sup>

additional classical exchange between b and the pair a/c takes place leading to line broadening and coalescence of all signals. By lineshape analysis we obtain  $\log A \approx 11$ ,  $E_a \approx 15 \text{ kJmol}^{-1}$  for the first and  $\log A \approx 13$ ,  $E_a \approx 20 \text{ kJmol}^{-1}$  for the second process.

The spectra in Fig.9 are noteworthy because of the size of  $J_{bc}$  which is much larger than expected for normal magnetic scalar couplings between hydrogen nuclei. Moreover,  $J_{bc}$  strongly increases with temperature from 50 Hz to more than 200 Hz. Unfortunately at higher temperatures the values of  $J_{bc}$  can no longer be extracted from the lineshape because of the hydrogen exchange processes. Even larger coupling constants  $J$  were observed for other transition metal hydrides.<sup>25-27</sup> Their origin has been explained in terms of a quantum exchange or coherent tunneling exchange process of hydrogen pairs according to Fig. 8d,<sup>25-30</sup> where the observed coupling constants (eg.  $J_{bc}$  in Fig.9) directly represent the average tunnel splittings of Fig.8d. Solvent interactions can be understood in terms of Fig.8f. The quantum exchange becomes an incoherent

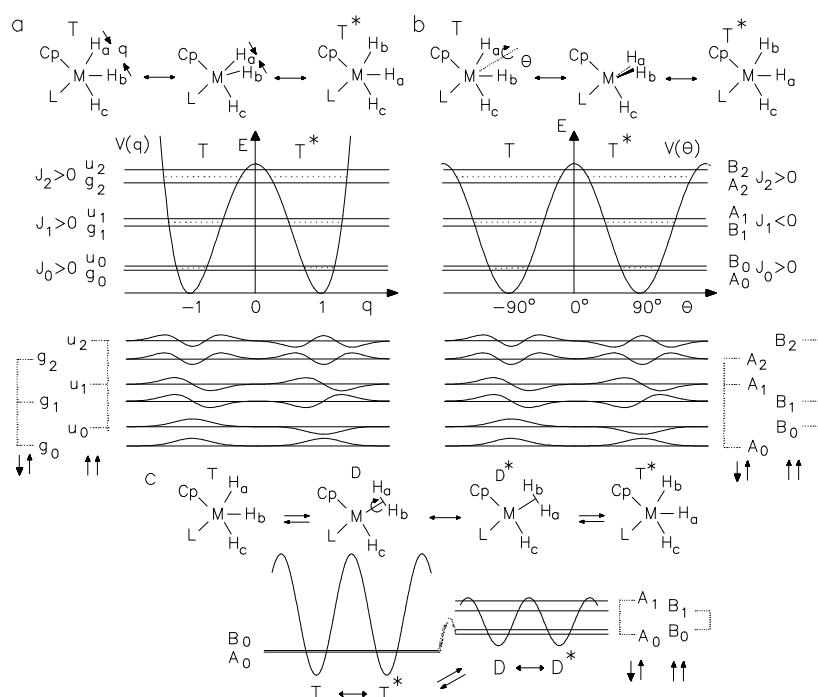


Fig.10. One-dimensional tunnel models<sup>30</sup> of the hydrogen exchange in metal trihydrides, ( $M = \text{Ru, Ir, Nb}$ ;  $\text{Cp} = \text{cyclopentadienyl}$ ,  $L = \text{Ligand}$ ) between the degenerate forms  $T$  and  $T^*$ . a: The reaction coordinate corresponds to the motion of the two hydrogen atoms along their internuclear distance vector  $q$ . b: The reaction coordinate corresponds to a rotation  $\theta$  of the internuclear distance vector around an axis in the  $\text{MH}_a\text{H}_b$ -plane. c: The reaction takes place in two steps: firstly, a metastable dihydrogen complex  $D$  is formed via an activated rate process; subsequently rotational tunneling takes place in  $D$ .

rate process at higher temperatures leading to the observed lineshape changes and prevents further study of the tunnel splittings.

Little is known about the details of the quantum tunnel process and the transition of the quantum versus the classical exchange process at higher temperatures. Fig.10 illustrates schematically different possible pathways of the quantum exchange.<sup>30</sup> In Fig.10a a hypothetical inversion pathway along a symmetric double minimum potential  $V(q)$  is shown, where  $q$  represents the

distance between the exchanging hydrogen atoms  $H_a$  and  $H_b$ . The states are then split as usual by tunneling, where the tunnel splittings  $J_n$  increase with vibrational energy. The different states are gerade or ungerade with respect to the inversion at  $q = 0$ . The g-states are linked according to the Pauli exclusion principle to the antisymmetric nuclear spin state ( $\uparrow\downarrow$ ) with antiparallel spins and the u-states to the symmetric nuclear states ( $\uparrow\uparrow$ ) with parallel spins. Vibrational relaxation takes place within the g- or within the u-states. Conversion of states with different symmetry is slow leading to average temperature dependent tunnel splittings  $J$ . As mentioned above, the latter appear as quantum coupling constants in the  $^1H$  NMR spectra. The increase of the observed coupling constants with temperature, e.g. of  $J_{bc}$  in Fig.9, arises then from an increase of the average tunnel splittings with energy assuming a Boltzmann distribution of states. In other words, NMR directly measures the tunnel splittings of the quantum exchange of hydrogen pairs in transition metal hydrides, averaged over different vibrational states and solvent configurations. Fig.10b shows a hypothetical rotational tunneling pathway involving a rotation angle  $\theta$  around an axis perpendicular to the  $H_a-H_b$  axis. In this case, the wave functions are either symmetric (A) or antisymmetric (B) with respect to the  $C_2$  operation. A has to be coupled to the antisymmetric ( $\uparrow\downarrow$ ) and B to the symmetric ( $\uparrow\uparrow$ ) nuclear spin functions leading to a sign alternance of the tunnel splittings which in turn leads to a decrease of the average tunnel splitting with temperature. This is not in agreement with the observed increase of  $J$  with temperature. Since the inversion process of Fig.10a is expected to involve a very high barrier, the pathway shown in Fig.10c has been proposed.<sup>19</sup> Here a stochastic process leads to a fast exchange of the trihydride state T with an intermediate dihydrogen state D in which rotational tunneling takes place. Since the population of D increases with temperature  $J$  also increases, as long as only the lowest splitting is important. Independent support for this mechanism comes from ab initio calculations of model compounds which find a metastable dihydrogen state D.<sup>29</sup>

In the future, both additional experimental and more sophisticated theoretical studies are necessary in order to understand these interesting phenomena.

## SUMMARY

It has been shown that dynamic high resolution liquid and solid state NMR spectroscopy can give interesting information about the elementary steps of proton transfer reactions which cannot easily be obtained using other methods. Although NMR is not the "fastest" kinetic method it is capable — using designed model systems — to contribute to the problem of how the environment changes the dynamics of hydrogen transfer processes. The results obtained may be of use for the development of theoretical reaction models for condensed phases.

## ACKNOWLEDGEMENTS

We thank the Deutsche Forschungsgemeinschaft, Bonn-Bad Godesberg, the European Community and the Fonds der Chemischen Industrie for financial support.

## REFERENCES

1. H.H.Limbach, Dynamic NMR Spectroscopy in the Presence of Kinetic Hydrogen/Deuterium Isotope Effects", in "NMR-Basic Principles and Progress", Vol. 23, p. 63-164, Springer, Heidelberg Berlin New-York 1991.
2. H.H.Limbach, J.Hennig, D.Gerritzen, H.Rumpel, Far.Discuss.Chem.Soc. 74 (1982) 822; D.Gerritzen, H.H.Limbach, J.Am.Chem.Soc. 106, 869

- (1984).
3. H.Rumpel, H.H.Limbach, *J.Am.Chem.Soc.* 111, 5429 (1989).
  4. M.Schlabach, H.Rumpel, H.H.Limbach, *Angew.Chem.* 101, 84 (1989);  
*Ang.Chem. Int.Ed.Engl.* 28, 76 (1989); M.Schlabach, G.Scherer,  
H.H.Limbach *J.Am.Chem.Soc.* 113, 3550 (1991).
  5. M.Schlabach, B.Wehrle, J.Braun, G.Scherer, H.H.Limbach,  
*Ber.Bunsenges.Phys.Chem.*, 96, 822 (1992).
  6. G.Otting, H.Rumpel, G.Scherer, H.H.Limbach, *Ber.Bunsenges.Phys.Chem.*  
90, 1122 (1986).
  7. G.Scherer, H.H.Limbach, *J.Am.Chem.Soc.* 111, 5946 (1989); G.Scherer,  
H.H.Limbach, submitted for publication.
  8. L.Meschede, D.Gerritzen, und H.H.Limbach, *Ber.Bunsenges.Phys.Chem.*  
92, 469 (1988); H.H.Limbach, L.Meschede, G.Scherer, *Z.Naturforsch.* 44a,  
459 (1989).
  9. L.Meschede, H.H.Limbach, *J.Phys.Chem.* 95, 10267 (1991).
  10. S.Nagoka, T.Terao, E.Imashiro, A.Saika, N.Hirota, S.Hayashi,  
*J.Chem.Phys.* 79, 4694 (1983).
  11. A.Heuer, U.Haeberlen, *J.Chem.Phys.*, 95, 4201 (1991).
  12. B.H.Meier, F.Graf, R.R.Ernst, *J.Chem.Phys.* 76, 767 (1982); R.Meyer,  
R.R.Ernst, *J.Chem.Phys.* 93, 5518 (1990).
  13. J.Schaeffer, E.O.Stejskal, *J.Am.Chem.Soc.* 98, 1031 (1976).
  14. H.H.Limbach, J.Hennig, R.D.Kendrick, C.S.Yannoni, *J.Am.Chem.Soc.*  
106, 4059 (1984).
  15. B.Wehrle, H.H.Limbach, M.Köcher, O.Ermer, E.Vogel, *Angew. Chem.* 99,  
914 (1987); *Angew.Chem.Int.Ed.Engl.* 26, 934 (1987).
  16. H.H.Limbach, B.Wehrle, H. Zimmermann, R.D.Kendrick, C.S.Yannoni, *J.*  
*Am. Chem.Soc.* 109, 929 (1987); H.H.Limbach, B.Wehrle,  
H.Zimmermann, R.D.Kendrick, C.S.Yannoni, *Angew. Chem.* 99, 241  
(1987); *Angew. Chem.Int.Ed.Engl.* 26, 247 (1987).
  17. H.H.Limbach, B.Wehrle, M.Schlabach, R.Kendrick, C.S.Yannoni,  
*J.Magn.Reson.* 77, 84 (1988).
  18. B.Wehrle, H.H.Limbach, H.Zimmermann, *J.Am.Chem.Soc.* 110, 7014  
(1988); B.Wehrle H.H.Limbach, *Chem.Phys.*, 136, 223 (1989).
  19. L.Frydman, A.C.Olivieri, A.E. Diaz, B.Frydman, F.G.Morin, C.L.Mayne,  
D.M.Grant, A.D.Adler, *J.Am.Chem.Soc.* 110, 8336 (1988); L.Frydman,  
A.C.Olivieri, A.E.Diaz, A. Valasinas; B.Frydman, *J.Am.Chem.Soc.* 110,  
5651 (1988).
  20. A.Baldy, J.Elguero, R.Faure, M.Pierrot, E.Vincent, *J.Am.Chem.Soc.* 107,  
5290 (1985); J.A.S.Smith, B.Wehrle, F.Aguilar-Parrilla, H.H.Limbach,  
M.C.Foces-Foces, F.H.Cano, J.Elguero, A.Baldy, M.Pierrot, M.M.Kurshid,  
J.B.Larcombe-McDouall, *J.Am.Chem.Soc.*, 111, 7304(1989).
  21. F.Aguilar-Parilla, G.Scherer, H.H.Limbach, M.C.Foces-Foces, F.H.Cano,  
J.A.S.Smith, C.Toiron, J.Elguero, *J.Am.Chem.Soc.*, 114, 9657 (1992).
  22. F.Aguilar-Parilla, H.H.Limbach, J.A.S.Smith, J.Elguero, unpublished.
  23. Ch.Hoelger, B.Wehrle, H.H.Limbach, submitted for publication.
  24. E.Bär, J.Fuchs, T.Kolrep D.Rieger, F.Aguilar—Parrilla, H.H.Limbach,  
W.P.Fehlhammer, *Angew.Chem.*, 103,88(1991).
  25. T.Arliguie, B.Chaudret, LDevillers, R.Poilblanc, R. C.R.Acad.Sci., Ser. 2  
305, 1523 (1987); A.Antinolo, B.Chaudret, G.Commenges, M.Fajardo,  
F.Jalon, R.H.Morris, A.Otero, C.T.Schweitzer, *J.Chem.,Soc.Chem.Comm.*  
1210 (1988); T.Arliguie, C.Border, B.Chaudret, J.Devillers, R.Poilblanc,  
*Organometallics*, 8,1308 (1989); R.R.Paciello, J.M.Manriquez, J.E.Bercaw,  
*Organometallics*, 9, 260 (1990); B.Chaudret, H.H.Limbach, C.Moise,  
*C.R.Acad.Sci. Paris, Ser. II*, 315, 533 (1992).

26. T.Arliguie, B.Chaudret, F.A.Jalon, A.Otero, J.A.Lopez, F.J.Lahoz, *Organometallics* 10, 1888 (1991);
27. D.M.Heinekey, N.G.Payne, G.K.Schulte, *J.Am.Chem.Soc.* 110, 2303 (1988); D.M.Heinekey, J.M.Millar, T.F.Koetzle, N.G.Payne, K.W.Zilm, *Am.Chem.Soc.* 112, 909 (1990); K.W.Zilm, D.M.Heinekey, J.M.Millar, N.G.Payne, P.Demou, *J.Am.Chem.Soc.* 111, 3088 (1989); K.W.Zilm, D.M.Heinekey, J.M.Millar, N.G.Payne, S.P. Neshyba, J.C.Duchamp, J.Szczyrba, *J.Am.Chem.Soc.* 112, 920 (1990); e: K.W.Zilm, J.M.Millar, *Adv.Magn.Reson.* 15, 163 (1990).
28. a: D.Jones, J.A.Labinger, J.Weitekamp, *J.Am.Chem.Soc.* 111, 3087 (1989); b: C.R.Bowers, D.H.Jones, N.D.Kurur, J.A.Labinger, M.G.Pravica, D.P.Weitekamp, *Adv.Magn.Reson.* 15, 269 (1990).
29. J.G.Barthelat, B.Chaudret, J.P.Dauby, Ph.De Loth, R.Poilblanc, *J.Am.Chem.Soc.* 113, 9896(1991).
30. H.H.Limbach, G.Scherer, M.Maurer, B.Chaudret, *Ang.Chemie*, 104, 1414 (1992); *Ang.Chem.Int.Ed.Engl.* 31, 1369 (1992)
31. R.P.Bell, *The Tunnel Effect in Chemistry*, Chapman and Hall, London 1980.
32. D.Borgis, J.T.Hynes, *J.Chem.Phys.* 94, 3619 (1990); D.Borgis, J.T.Hynes, *J.Chem.Phys.* 170, 315 (1993).
33. G.Zundel, M.Eckert, *J.Mol.Struct.* 200, 73 (1989) and references cited therein; E.Grech, Z.Malaarski, M.Ilczyzyn, O.Czupinski, L.Sobczyk, J.Rozière, B.Bonnet, J.Potier, *J.Mol.Struct.*, 128, 249 (1985).
34. P.M.Morse, E.C.G.Stückelberg, *Helv.Phys.Acta* 4, 337(1931); R.L.Somorjai, D.F.Hornig, *J.Phys.Chem.* 36, 1980 (1962); J.Brickmann, H.Zimmermann, *Ber. Bunsenges. Phys. Chem.* 70, 157 (1966); d: *ibid.* 70, 521 (1966) 521; e: *ibid.* 71, 160 (1967); *J.Chem.Phys.* 50, 1608 (1969); f: J.Brickmann, H.Zimmermann *Z.f.Naturf.* 23a, 11(1968); g: J.Laane, *Applied Spectroscopy*, 24, 73 (1970).
35. J.D.McDonald, *Ann.Rev.Phys.Chem.* 30, 29 (1972).
36. W.F.Rowe, R.W.Duerst, E.B.Wilson, *J.Am.Chem.Soc.* 98, 4021 (1976); S.L.Baughcum, R.W.Duerst, W.F.Rowe, Z.Smith, E.B.Wilson, *J.Am.Chem.Soc.* 103, 6296 (1981); S.L.Baughcum, Z.Smith, E.B.Wilson, R.W.Duerst, *J.Am.Chem.Soc.* 106, 2260 (1984).
37. D.W.Firth, P.F.Barbara, H.P.Trommsdorf, *Chem.Phys.* 136, 349 (1989).
38. E.Bosch, M.Moreno, J.M.Lluch *JACS* 114 2072 (1992).
39. G.Scherer, B.Chaudret, H.H.Limbach, unpublished.